J. Am. Chem. Soc. **1994**, *116*, 2409–2417

Formation, Structures, and Reactions of Calcium and Barium Mono(alkoxide) Complexes

Kris F. Tesh, David J. Burkey, and Timothy P. Hanusa[*]

Contribution from the Department of Chemistry, Vanderbilt University, Nashville, Tennessee 37235

Received September 13, 1993[⊗]

Abstract: Calcium diiodide dissolves in THF to produce the tetrasolvated octahedral complex $CaI_2(THF)_4$ (**1**). The complex crystallizes in the space group $P2_1/c$ with a = 8.201(7) Å, b = 14.262(9) Å, c = 10.008(6) Å, β = 93.93(6)° and D_c = 1.656 g/cm^3 for Z = 2. The iodide ligands are *trans* to each other with Ca–I bond distances of 3.106(2) Å. CaI_2 reacts with 1 equiv of $K[OC(C_6H_5)_2CH_2C_6H_4\text{-}Cl\text{-}4]$ (=Kclox) in THF to produce the mono(alkoxide) complex $ICa(clox)(THF)_4$ (**2**). The mono(alkoxide) is also produced by the conproportionation of $Ca(clox)_2(THF)_3$ and CaI_2 in THF. It crystallizes from THF in the space group $P\bar{1}$ with a = 10.547(3) Å, b = 19.537(5) Å, c = 10.343(3) Å, α = 90.54(2)°, β = 93.93(6)°, γ = 103.60(2)°, and D_c = 1.387 g/cm^3 for Z = 2. The geometry around the calcium in $ICa(clox)(THF)_4$ is a distorted octahedron, with the iodide and alkoxide in a *cis* arrangement: Ca–I = 3.108(3) Å and Ca–OR = 2.097(7) Å. $ICa(clox)(THF)_4$ can be derivatized in THF with K(clox) and $KN(SiMe_3)_2$ to yield $Ca(clox)_2(THF)_3$ and $(clox)Ca[N(SiMe_3)_2](THF)_3$ (**3**), respectively. The latter is the first example of a monomeric calcium complex containing both monodentate alkoxide and amide ligands. It crystallizes in the space group $P\bar{1}$ with a = 12.298(4) Å, b = 17.025(4) Å, c = 10.958(3) Å, α = 91.04(2)°, β = 114.88(2)°, γ = 89.57(2)°, and D_c = 1.156 g/cm^3 for Z = 2. $(clox)Ca[N(SiMe_3)_2](THF)_3$ has a distorted trigonal bipyramidal geometry, with THF ligands occupying axial sites: Ca–N = 2.353(3) Å and Ca–OR = 2.087(4) Å. BaI_2 will react with $K[OC_6H_2\text{-}t\text{-}Bu_2\text{-}2,6\text{-}Me\text{-}4]$ (=KBHT) in THF to form the mono(aryloxide) complex $[IBa(BHT)(THF)_3]_2$ (**4**). It is also formed from the conproportionation of BaI_2 and $Ba(BHT)_2(THF)_3$ in THF. The compound crystallizes as an iodide-bridged dimer, $[Ba(\mu\text{-}I)(BHT)(THF)_3]_2\cdot(THF)_2$, with two lattice THF molecules per dimer. The space group is $P2_1/c$, with a = 13.997(4) Å, b = 14.164(8) Å, c = 18.161(4) Å, β = 104.26(2)°, and D_c = 1.469 g/cm^3 for Z = 2 (dimers). The barium atoms have a distorted octahedral coordination geometry, with Ba–I (I′) = 3.442(2) (3.590(2)) Å and Ba–OAr = 2.408(8) Å. $[IBa(BHT)(THF)_3]_2$ will react with KBHT in THF to form the known bis(alkoxide) $Ba(BHT)_2(THF)_3$. Both $ICa(clox)(THF)_4$ and $[IBa(BHT)(THF)_3]_2$ are stable toward disproportionation in THF. Stirring $[IBa(BHT)(THF)_3]_2$ in toluene removes the THF ligands and produces the insoluble oligomer $[IBa(BHT)]_n\,(C_7H_8)_x$, whereas $ICa(clox)(THF)_4$ slowly decomposes in aromatics to give primarily the bis(alkoxide) $[Ca(\mu\text{-}clox)(clox)(THF)]_2$ and $CaI_2(THF)_x$. The metal coordination numbers for the mono(alkoxides), which are often less than might be expected from steric considerations, suggest that the Lewis acidity of the metal center influences the extent of solvation in alkoxide complexes.

Introduction

Apart from recent interest in their use as precursors to metal oxides via sol-gel or chemical vapor deposition techniques,[1,2] alkaline-earth (Ae) alkoxides are notable for their rich, even bewildering, variety of structures and reactions.[3] Crystallographically identified structural types range from discrete monomeric species such as $Sr[OC_6H_2(t\text{-}Bu)_3]_2(THF)_3$[4] and $Ca[OC(C_6H_5)_2CH_2C_6H_4\text{-}Cl\text{-}4]_2(THF)_3$[5] to large polynuclear aggregates such as $Ba_6O(OC_2H_4OMe)_{10}(HOC_2H_4OMe)_4$[6] and $Ca_9(OCH_2CH_2OMe)_{18}(HOCH_2CH_2OMe)_2$.[7] Owing to the wide range of ligands that have been used and to the conformational and bonding flexibility of the alkoxide ligand (e.g., μ^1-, μ^2-, and μ^3-bonding modes are known), unifying structural principles for alkaline-earth alkoxides have been slow to emerge.[5] Similarly, their complex solution behavior has hindered attempts to construct a consistent picture of alkoxide reactivity; for example, the controlled hydrolysis of alkaline-earth metal-alkoxide bonds remains a challenging problem.[8,9]

In contrast to the recent surge in research with Group 2 bis(alkoxides), the analogous *mono*(alkoxide) species $[(ROAeX(L)_n)]$ (X = monovalent anion; L = neutral base) have been far less studied. They are a conceptually interesting class of compounds, however, as they combine alkoxides with other anionic ligands, such as halides, amides, and hydrocarbyls to form heteroleptic alkaline-earth alkoxide complexes. They offer an attractive means to study the relative bonding strength for different ligands and the tendency of specific ligands to bridge in polymetallic systems.[10] The appropriate mono(alkoxides) also might be derivatized with different alkoxide ligands, leading to mixed (RO)Ae(OR′) species. Mono(alkoxide) halides can be considered intermediates in the formation of bis(alkoxides) from AeX_2 complexes, and hence their study also could lead to new insights into the formation and reactivity of the bis(alkoxides).

A variety of mono(alkoxides) and siloxides of beryllium and magnesium have been reported, and several have been structurally characterized, including $[Be(Me)(OSiMe_3)]_4$,[11] $[BeBr(\mu\text{-}O\text{-}t\text{-}Bu)(Et_2O)]_2$,[12] $[MgBr(O\text{-}t\text{-}Bu)(Et_2O)]_2$,[13] the bromoenolate $[CH_3CH{=}C(t\text{-}Bu)OMgBr]_2\cdot(THF)_2$,[14] and the tetrameric cy-

---

[⊗] Abstract published in *Advance ACS Abstracts*, February 15, 1994.

(1) Hubert-Pfalzgraf, L. G. *Nouv. J. Chem.* **1987**, *11*, 663–675.

(2) Bradley, D. C. *Chem. Rev.* **1989**, *89*, 1317–1322.

(3) Hanusa, T. P. *Chem. Rev.* **1993**, *93*, 1023–1036.

(4) Drake, S. R.; Otway, D. J.; Hursthouse, M. B.; Abdul Malik, K. M. *Polyhedron* **1992**, *11*, 1995–2007.

(5) Tesh, K. F.; Hanusa, T. P.; Huffman, J. C.; Huffman, C. J. *Inorg. Chem.* **1992**, *31*, 5572–5579.

(6) Caulton, K. G.; Chisholm, M. H.; Drake, S. R.; Huffman, J. C. *J. Chem. Soc., Chem. Commun.* **1990**, 1498–1499.

(7) Goel, S. C.; Matchett, M. A.; Chiang, M. Y.; Buhro, W. E. *J. Am. Chem. Soc.* **1991**, *113*, 1844–1845.

(8) Hench, L. L.; West, J. K. *Chem. Rev.* **1990**, *90*, 33–72.

(9) Sanchez, C.; Livage, J. *Nouv. J. Chem.* **1990**, *14*, 513–521.

(10) McGeary, M. J.; Folting, K.; Caulton, K. G. *Inorg. Chem.* **1989**, *28*, 4051–4053.

(11) Mootz, D.; Zinnius, A.; Böttcher, B. *Angew. Chem., Int. Ed. Engl.* **1969**, *8*, 378–379.

0002-7863/94/1516-2409$04.50/0

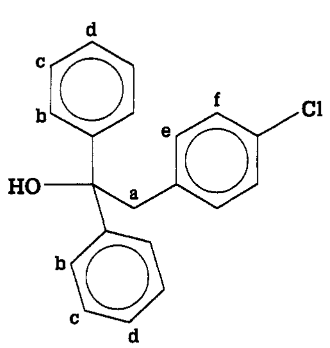

Figure 1. Labeling scheme for the Hclox protons.

clopentadienyl alkoxide $[CpMgOEt]_4$.[15] In contrast, we have found only one previous report on mono(alkoxide) complexes of calcium; it describes the synthesis of a series of ROCaCl compounds from the reaction of $(Ph_3C)CaCl(THF)_2$ with alcohols (eq 1).[16] The mono(alkoxides) were characterized solely by

$$(Ph_3C)CaCl + ROH \rightarrow ROCaCl + Ph_3CH \qquad (1)$$
$$R = Me, Et, Bu, Ph, p\text{-}ClC_6H_4, p\text{-}NO_2C_6H_4$$

elemental analysis, and no subsequent reactions or structural details were reported for them. Analogous mono(alkoxide) compounds containing Sr or Ba have not been reported. Our previous success in preparing bis(alkoxides) via halide metathesis[5] led us to extend this method to mono(alkoxide) complexes. We report here the synthesis and first structural characterization of a calcium mono(alkoxide) halide and a barium mono(aryloxide) halide and examples of their derivatization chemistry.

Experimental Section

General Experimental Considerations. All manipulations were performed with the rigid exclusion of air and moisture using high-vacuum, Schlenk, or drybox techniques. Proton NMR spectra were obtained at 300 MHz with a Bruker NR-300 spectrometer and were referenced to the residual proton resonances of C_6D_6 (δ 7.15) or THF-d_8 (δ 3.58); carbon (^{13}C) NMR spectra were recorded at 50.3 or 75.5 MHz on AC-200 or NR-300 spectrometers, respectively, and were referenced to the residual ^{13}C resonances of THF-d_8 (δ 67.4). The labelling scheme for the hydrogen atoms of the $HOC(Ph_2)_2CH_2C_6H_4$-Cl-4 (Hclox) ligand is given in Figure 1. Infrared data were obtained on a Perkin-Elmer 1600 Series FT-IR spectrometer; the KBr pellets were prepared as previously described.[17] Elemental analyses were performed by Oneida Research Services, Whitesboro, NY.

Materials. Anhydrous calcium iodide and barium iodide (95%) were commercial samples (Strem Chemicals or Cerac) heated under vacuum to remove residual amounts of free iodine. Potassium hydride was obtained from Strem Chemicals or Aldrich as a dispersion in oil and was washed with hexane and dried before use. $KN(SiMe_3)_2$, HOC_6H_2-*t*-Bu_2-2,6-Me-4 (referred to as HBHT), and $HOC(Ph_2)_2CH_2C_6H_4$-Cl-4 (referred to as Hclox) were purchased from Aldrich and used without further purification. $Ca(clox)_2(THF)_3$ and $Ba(BHT)_2(THF)_3$ were prepared as previously described.[5] Solvents for reactions were distilled under nitrogen from sodium or potassium benzophenone ketyl. NMR solvents were vacuum distilled from Na/K (22/78) alloy and stored over 4A molecular sieves prior to use.

Preparation of $CaI_2(THF)_4$ (1). Anhydrous CaI_2 was dissolved in THF. Crystals of **1** were grown by slow evaporation of the solvent over several days. A suitable crystal chosen for X-ray structure analysis confirmed the degree of solvation reported previously.[18]

Preparation of ICa(clox)(THF)$_4$ (2). Method A: KH (40 mg, 1.0 mmol) and Hclox (0.307 g, 0.99 mmol) were added to a 125-mL Erlenmeyer flask. THF (70 mL) was added, and the mixture was stirred for 15 min, during which time H_2 was evolved and the solution became yellow. CaI_2 (0.297 g, 1.01 mmol) was added to the reaction; a copious amount of a white precipitate appeared within seconds. The solution was stirred overnight and then allowed to settle. The clear supernatant liquid was removed by pipet and was evaporated to a volume of about 2 mL. Upon slow evaporation of the remaining solvent, a crop of clear crystals of **2** was obtained that weighed 0.748 g (90% yield). Anal. Calcd for $C_{36}H_{48}CaClIO_5$: C, 56.65; H, 6.34; Ca, 5.25; I, 16.63. Found: C, 56.85; H, 6.33; Ca, 4.92; I, 16.72. ^1H NMR (THF-d_8): δ 7.40 (d, J = 7.3 Hz, 4H, H_b); 7.09 (t, J = 7.3 Hz, 4H, H_c); 6.98 (t, J = 7.1 Hz, 2H, H_d); 6.90 (d, J = 7.1 Hz, 2H, H_f); 6.83 (d, J = 8.2 Hz, 2H, H_e); 3.61 (t, J = 6.5 Hz, α-C_4H_8O); 3.48 (s, 2H, H_a); 1.77 (m, 16H, β-C_4H_8O). ^{13}C NMR (THF-d_8): δ 155.9 (Ar-*C*Cl); 140.9 (Ar-*C*R); 133.4 (Ar-*C*H); 130.9 (Ar-*C*R); 128.4 (Ar-*C*H); 127.3 (Ar-*C*H); 125.2 (Ar-*C*H); 82.1 (*C*–O); 68.2 (α-C_4H_8O); 51.3 (CH_2); 26.3 (β-C_4H_8O). Principal IR bands (KBr pellet, cm^{-1}): 3052, w; 2975, s; 2879, s; 1595, w; 1490, s; 1460, m; 1443, m; 1404, w; 1293, m; 1206, w; 1174, m; 1121, s; 1089, m; 1067, m; 1037, s, vbr; 953, w; 883, s, br; 824, m; 778, m; 753, m; 727, m; 703, s; 668, m; 628, m; 606, m; 581, w; 514, w; 456, m. Slow recrystallization from THF produced crystals of **2** that were used for X-ray structural analysis.

Method B: CaI_2 (0.18 g, 0.613 mmol) was dissolved in 40 mL of THF. $Ca(clox)_2(THF)_3$ (0.533 g, 0.611 mmol) was added to the solution; within seconds the dissolution was complete. Removal of the THF under vacuum to a volume of 5 mL, followed by slow evaporation of the remaining solvent at ambient pressures, resulted in the nearly quantitative isolation of crystalline **2** (0.38 g, 98% yield), as determined by ^1H NMR (THF-d_8).

Preparation of Ca(clox)$_2$(THF)$_3$ from Kclox and 2. KH (40 mg, 1.00 mmol) and Hclox (0.266 g, 0.86 mmol) were stirred for 1 h in 20 mL of THF. H_2 gas evolved from the reaction, and the solution turned a transparent green color. ICa(clox)(THF)$_4$ (0.550 g, 0.86 mmol) was then added, and a white precipitate formed immediately in the solution. The reaction mixture was stirred overnight and then set aside to settle. The clear THF solution was separated from the precipitate with a pipet. The solvent volume was reduced to ca. 5 mL under vacuum, and then then the solvent was allowed to evaporate slowly at ambient pressure to yield 0.57 g (76% yield) of $Ca(clox)_2(THF)_3$ as colorless crystals, as confirmed by ^1H NMR (C_6D_6).

Preparation of (clox)Ca[N(SiMe$_3$)$_2$](THF)$_3$ (3). $KN(SiMe_3)_2$ (0.198 g, 1.00 mmol), **2** (0.762 g, 1.00 mmol), and 50 mL of THF were stirred overnight, producing a white precipitate and a golden solution. The solution was then allowed to settle, and the yellow supernatant liquid was removed by decantation. The THF was removed under vacuum until the volume was reduced to 2 mL; the remaining solvent was allowed to evaporate slowly at ambient pressure, leaving 0.653 g (90% yield) of **3** as colorless crystals. Anal. Calcd for $C_{38}H_{58}CaClNO_4Si_2$: C, 62.99; H, 8.07; N, 1.93. Found: C, 62.65; H, 7.67; N, 1.51. ^1H NMR (THF-d_8): δ 7.51 (d, J = 7.4 Hz, H_b); 7.36 (d, J = 7.4 Hz, H_b); 7.10 (t, J = 7.5 Hz, H_c); 6.99 (t, J = 7.1 Hz, H_c); 6.90–6.72 (several overlapping H_d, H_e, and H_f doublets); 3.62 (m, 12 H, α-C_4H_8O); 3.52 (s, H_a); 3.47 (s, H_a); 1.77 (m, 12 H, β-C_4H_8O); 0.01 (s, $Si(CH_3)_3$); –0.02 (s, $Si(CH_3)_3$). Two sets of resonances (**3a**, **3b**) were evident in the C_6D_6 ^1H NMR spectrum: δ 7.53 (d, J = 7.1 Hz, **3a**); 7.40 (d, J = 7.3 Hz, **3b**); 7.35 (d, J = 7.3 Hz, **3a**); 7.20–6.89 (several overlapping peaks); 6.70 (d, J = 8.4 Hz, **3b**); 6.58 (d, J = 8.4 Hz, **3a**); 3.69 (s, H_a, **3b**); 3.53 (s, H_a, **3a**); 3.45 (t, J = 6.5 Hz, α-C_4H_8O); 1.33 (m, β-C_4H_8O); 0.54 (s, $Si(CH_3)_3$, **3a**); 0.36 (s, $Si(CH_3)_3$, **3a**); 0.21 (s, $Si(CH_3)_3$, **3b**); 0.18 (s, $Si(CH_3)_3$, **3b**). The **3a** set of peaks increases and the **3b** set of peaks decreases in intensity if the concentration of **3** is increased. Variable amounts of $Ca(clox)_2(THF)_3$[5] and $Ca[N(SiMe_3)_2](THF)_2$[19] were also present in the C_6D_6 NMR spectrum of **3**; their area never represented more than approximately 5% of the total of **3a** and **3b**. ^{13}C NMR (THF-d_8): δ 156.7 (Ar-*C*Cl); 155.5 (Ar-*C*Cl); 141.4 (Ar-*C*R); 140.9 (Ar-*C*R); 133.6 (Ar-*C*R); 133.2 (Ar-*C*H); 133.1 (Ar-*C*H); 129.1 (Ar-*C*R); 128.6 (Ar-*C*H); 128.3 (Ar-*C*R); 127.9 (Ar-*C*H); 127.5 (Ar-*C*H); 127.4 (Ar-*C*H); 125.3 (Ar-*C*H); 125.1 (Ar-*C*H); 82.4 (*C*–O); 81.0 (*C*–O); 68.2 (α-C_4H_8O); 51.5 (CH_2); 51.2 (CH_2); 26.4 (β-C_4H_8O); 6.2 ($Si(CH_3)_3$); 6.1 ($Si(CH_3)_3$). Principal IR bands (KBr pellet, cm^{-1}): 2945, s; 2879, s; 1595, w; 1491, s; 1444, m; 1406, w; 1295, w; 1229, s; 1180, w; 1132, s; 1048, s, br; 956, w; 880, s; 822, s; 784, m; 756, m; 726, m; 701, s; 657, m; 628, w; 608, w; 456, m.

---

[12] Bell, N. A.; Shearer, H. M. M.; Twiss, J. *Acta Crystallogr., Sect. C* **1984**, *40*, 605–607.

[13] Bell, N. A.; Moseley, P. T.; Shearer, H. M. M. *Acta Crystallogr., Sect. C* **1984**, *40*, 602–604.

[14] Williard, P. G.; Salvino, J. M. *J. Chem. Soc., Chem. Commun.* **1986**, 153–154.

[15] Lehmkuhl, H.; Mehler, K.; Benn, R.; Rufinska, A.; Krueger, C. *Chem. Ber.* **1986**, *119*, 1054–1069.

[16] Masthoff, R.; Krieg, G.; Vieroth, C. *Z. Anorg. Allg. Chem.* **1969**, *364*, 316–321.

[17] Williams, R. A.; Tesh, K. F.; Hanusa, T. P. *J. Am. Chem. Soc.* **1991**, *113*, 4843–4851.

[18] McCormick, M. J.; Sockwell, S. C.; Davies, C. E. H.; Hanusa, T. P.; Huffman, J. C. *Organometallics* **1989**, *8*, 2044–2049.

[19] Westerhausen, M. *Inorg. Chem.* **1991**, *30*, 96–101.

Table 1. Crystal Data and Summary of X-ray Data Collection

compound	**1**	**2**	**3**	**4**
formula	$C_{16}H_{32}CaI_2O_4$	$C_{36}H_{48}CaClIO_5$	$C_{38}H_{58}CaClNSi_2O_4$	$C_{31}H_{55}BaIO_5$
fw	582.32	763.21	724.58	772.01
color of crystal	colorless	colorless	colorless	colorless
cryst dimens, mm	0.20 × 0.20 × 0.20	0.20 × 0.30 × 0.45	0.40 × 0.50 × 0.20	0.10 × 0.20 × 0.30
space group	$P2_1/c$	$P\bar{1}$	$P\bar{1}$	$P2_1/c$
temperature (°C)	20	20	20	-100
a, Å	8.201(7)	10.547(3)	12.298(4)	13.997(4)
b, Å	14.262(9)	19.537(5)	17.025(4)	14.164(8)
c, Å	10.008(6)	10.343(3)	10.958(3)	18.161(4)
α, deg		90.54(2)	91.04(2)	
β, deg	93.93(6)	117.06(2)	114.88(2)	104.26(2)
γ, deg		103.60(2)	89.57(2)	
V, Å^3	1168(2)	1827.9(9)	2081(2)	3489(4)
Z	2	2	2	2 (dimers)
D (calcd), g/cm^3	1.656	1.387	1.156	1.469
abs coeff, cm^{-1}	28.9	11.13	3.0	20.4
transmission factors	0.70–1.00	0.89–1.00	no correction	0.85–1.00
scan speed, deg/min	8.0	4.0	4.0	8.0
scan width	$1.73 + 0.30 \tan \theta$	$1.15 + 0.30 \tan \theta$	$1.15 + 0.30 \tan \theta$	$1.37 + 0.30 \tan \theta$
total reflections	2295	7197	8863	6709
unique reflections	2143	6468	7349	6436
no. with $F > 3.0\sigma(F)$	819	2276	2725	2829
$R(F)$	0.060	0.052	0.055	0.055
$R_w(F)$	0.070	0.058	0.064	0.071
goodness of fit	2.36	1.62	1.78	1.85
max Δ/σ in final cycle	0.01	0.02	0.09	0.14
max peak (final diff map) (e$^-$/Å^3)	1.13	0.58	0.25	1.32

Preparation of $[IBa(BHT)(THF)_3]_2$ (4). Method A: KH (47 mg, 1.17 mmol) and HBHT (0.222 g, 1.01 mmol) were stirred in 60 mL of THF for 10 min; H_2 was evolved and a clear, light-yellow solution formed. Addition of BaI_2 (0.410 g, 1.05 mmol) led to the immediate formation of a white precipitate. The cloudy white solution was stirred overnight and set aside to allow the precipitate to settle. The clear supernatant solution was then decanted, and THF was removed under vacuum until the volume was reduced to ca. 2 mL. Further slow evaporation at ambient pressure resulted in the isolation of 0.641 g (92% yield) of **4** as colorless crystals. Anal. Calcd for $C_{27}H_{47}BaIO_4$: C, 46.33; H, 6.77; Ba, 19.62. Found: C, 47.03; H, 6.64; Ba, 19.96. ^1H NMR (THF-d_8): δ 6.68 (s, 2H, Ar-H); 3.61 (t, J = 6.5 Hz, 12H, α-C_4H_8O); 2.09 (s, 3H, Ar-CH_3); 1.77 (m, 12H, β-C_4H_8O); 1.43 (18H, Ar-$C(CH_3)_3$). ^{13}C NMR (THF-d_8): δ 136.3 (Ar-2,6); 125.1 (Ar-3,5); 117.8 (Ar-4); 35.3 (Ar-$C(CH_3)_3$); 30.9 (Ar-$C(CH_3)_3$); 21.6 (Ar-CH_3). Principal IR bands (KBr pellet, cm^{-1}): 2950, s, br; 1458, m; 1420, s; 1380, m; 1344, w; 1278, s; 1216, w; 1198, w; 1040, s; 880, m; 819, m; 801, m; 497, m. The acquisition of NMR data for **4** in C_6D_6 is precluded by its insolubility in aromatics (see Results section).

Method B: BaI_2 (0.194 g, 0.50 mmol) was stirred in THF (50 mL) for several hours; the dissolution was incomplete. When $Ba(BHT)_2(THF)_3$ (0.392 g, 0.49 mmol) was added, within minutes dissolution of the two solids occurred and a clear homogeneous solution resulted. The solvent was evaporated to dryness, leaving colorless crystals of **4** in quantitative yield, as confirmed by its ^1H NMR spectrum (THF-d_8) and its lack of solubility in aromatics (see Results section).

Preparation of $[IBa(BHT)]_n(C_7H_8)_x$ (5). **4** (1.14 g, 1.63 mmol) was added to 30 mL of toluene, and the resulting gray suspension was stirred overnight. During this time, the suspension thickened noticeably. The suspension was filtered through a medium glass frit, and the retained solid was dried for 2 h under vacuum to yield 0.84 g of a dense, gray solid (**5**). No product was isolated on removal of the toluene from the filtrate, demonstrating that none of **4** had dissolved in the toluene. Dissolving **5** in THF cleanly regenerated **4** (determined by ^1H NMR). This behavior, coupled with spectroscopic analysis, lead to the identification of **5** as $[IBa(BHT)]_n(C_7H_8)_x$. Principal IR bands (KBr pellet, cm^{-1}): 2952, s; 1458, m; 1411, s; 1382, m; 1341, w; 1264, m; 1233, s; 1212, s; 1028, m; 788, s; 464, w. Nonstoichiometric quantities of toluene were always present in isolated samples of **5**, which could not be completely removed, even on prolonged drying under vacuum; because of this, elemental analysis data for **5** were not obtained.

Preparation of $Ba(BHT)_2(THF)_3$ from KBHT and 4. KH (49 mg, 1.22 mmol) and HBHT (0.221 g, 1.00 mmol) were stirred for 60 min in 30 mL THF, during which time H_2 gas evolved and a clear, yellow solution formed. **4** (0.701 g, 1.00 mmol) was then added, and a white precipitate immediately formed. The reaction mixture was stirred overnight and then set aside to allow the precipitate to settle. The clear filtrate was separated by decantation and the volume reduced to ca. 10 mL under vacuum. The remaining THF was allowed to evaporate slowly at ambient pressure, leaving 0.688 g (87% yield) of $Ba(BHT)_2(THF)_3$ as a white powder. The identity of the solid was confirmed by ^1H NMR (C_6D_6).[5]

General Procedures for X-ray Crystallography. A suitable crystal of each compound was located and sealed in a quartz capillary tube, except for **4**, which was mounted on a glass fiber and placed directly in a nitrogen gas cold stream. All measurements were performed on a Rigaku AFC6S diffractometer at Vanderbilt University with graphite monochromated Mo-Kα radiation (λ = 0.71069 Å). Relevant crystal and data collection parameters for the present study are given in Table 1.

Cell constants and orientation matrices for the data collection were obtained from least-squares refinements using the setting angles of 22–25 accurately centered reflections. Data collection was performed between the limits $6° \leq 2\theta \leq 50°$ using continuous $\omega - 2\theta$ scans with stationary backgrounds (peak/bkgd counting time = 2/1). The intensities of three representative reflections measured after every 150–200 reflections declined by 8% for **2**; in this case, a correction was applied to the data to account for the decay. The other crystals displayed no decay. The space groups were determined from packing considerations, statistical analyses of intensity distribution, and where appropriate, systematic absences. Subsequent solution and refinement of the structures confirmed the choice in each case. Data were reduced to a unique set of intensities and associated σ values in the usual manner. The structures were solved by direct methods (SHELXS-86) and Fourier techniques. Where required, an empirical absorption correction was applied, based on azimuthal scans of several reflections. All non-hydrogen atoms were refined anisotropically. To improve the refinement of the non-hydrogen atoms, hydrogen atoms were inserted in calculated positions based on packing considerations and d(C–H) = 0.95 Å. The positions were fixed for the final cycle of refinement. Final difference maps were essentially featureless. Selected bond distances and angles are listed in Tables 2–5.

Results

Synthesis of Mono(alkoxide) Iodides. Two mono(alkoxide) iodide complexes of a heavy alkaline-earth metal have been prepared in this study, $ICa(clox)(THF)_4$ (**2**) and $[IBa(BHT)(THF)_3]_2$ (**4**).[20] Both can be formed by two different routes: (1) a metathetical route employing a 1/1 reaction of a potassium alkoxide and an alkaline-earth diiodide (eq 2) and (2) a conproportionation reaction of the corresponding bis(alkoxide) species and an alkaline-earth diiodide (eq 3). The reactions are conducted in THF; there is no evidence of subsequent disproportionation of the mono(alkoxides) in this solvent (e.g., as in eq

---

[20] Both alkoxides and aryloxides will be referred to as "alkoxides", unless it is important to distinguish them.

Table 2. Summary of Bond Lengths (Å) and Angles (deg) in CaI$_2$(THF)$_4$

Ca–I	3.106(2) Å
Ca–O (av)	2.34(1) Å
I–Ca(1)–I′	180.00°
I–Ca–O (av)	90.0(6)°
O(1)–Ca–O(1)′	180.00°
O(1)–Ca–O(2) (av)	90.0(7)°

Table 3. Summary of Bond Lengths (Å) and Angles (deg) in ICa(clox)(THF)$_4$

	Distances		
I(1)–Ca(1)	3.108(3)	Ca(1)–O(33)	2.433(8)
Ca(1)–O(2)	2.097(7)	Ca(1)–O(38)	2.391(9)
Ca(1)–O(23)	2.434(9)	Cl(1)–C(8)	1.74(1)
Ca(1)–O(29)	2.454(9)	O(2)–C(3)	1.37(1)
	Angles		
I(1)–Ca(1)–O(2)	98.8(2)	O(2)–Ca(1)–O(38)	97.5(3)
I(1)–Ca(1)–O(23)	166.5(2)	O(23)–Ca(1)–O(29)	80.3(3)
I(1)–Ca(1)–O(29)	86.7(2)	O(23)–Ca(1)–O(33)	89.6(3)
I(1)–Ca(1)–O(33)	92.0(2)	O(23)–Ca(1)–O(38)	83.7(4)
I(1)–Ca(1)–O(38)	92.1(3)	O(29)–Ca(1)–O(33)	82.2(3)
O(2)–Ca(1)–O(23)	94.5(3)	O(29)–Ca(1)–O(38)	86.5(3)
O(2)–Ca(1)–O(29)	173.1(3)	O(33)–Ca(1)–O(38)	167.7(3)
O(2)–Ca(1)–O(33)	93.3(3)	Ca(1)–O(2)–C(3)	172.9(6)

Table 4. Summary of Bond Lengths (Å) and Angles (deg) in (clox)Ca[N(SiMe$_3$)$_2$](THF)$_3$

	Distances		
Ca(1)–O(2)	2.087(4)	Cl(1)–C(8)	1.744(8)
Ca(1)–O(29)	2.460(5)	Si(1)–N(1)	1.682(5)
Ca(1)–O(34)	2.399(5)	Si(2)–N(1)	1.682(5)
Ca(1)–O(39)	2.398(5)	O(2)–C(3)	1.369(7)
Ca(1)–N(1)	2.353(5)		
	Angles		
O(2)–Ca(1)–O(29)	100.6(2)	O(34)–Ca(1)–O(39)	159.1(2)
O(2)–Ca(1)–O(34)	97.5(2)	O(34)–Ca(1)–N(1)	90.3(2)
O(2)–Ca(1)–O(39)	97.5(2)	O(39)–Ca(1)–N(1)	93.3(2)
O(2)–Ca(1)–N(1)	124.2(2)	Ca(1)–O(2)–C(3)	169.1(4)
O(29)–Ca(1)–O(34)	82.8(2)	Ca(1)–N(1)–Si(1)	114.6(3)
O(29)–Ca(1)–O(39)	80.2(2)	Ca(1)–N(1)–Si(2)	121.5(3)
O(29)–Ca(1)–N(1)	135.2(2)	Si(1)–N(1)–Si(2)	123.8(3)

Table 5. Summary of Bond Lengths (Å) and Angles (deg) in [IBa(BHT)(THF)$_3$]$_2$

	Distances		
Ba(1)–I(1)	3.442(2)	Ba(1)–O(23)	2.70(1)
Ba(1)–I(1)′	3.590(2)	Ba(1)–O(28)	2.70(1)
Ba(1)–O(2)	2.408(8)	O(2)–C(3)	1.35(2)
Ba(1)–O(18)	2.71(1)		
	Angles		
I(1)–Ba(1)–I(1)′	75.77(4)	O(2)–Ba(1)–O(18)	101.4(3)
I(1)–Ba(1)–O(2)	109.0(3)	O(2)–Ba(1)–O(23)	84.7(3)
I(1)–Ba(1)–O(18)	149.5(2)	O(2)–Ba(1)–O(28)	87.9(3)
I(1)–Ba(1)–O(23)	97.4(3)	O(18)–Ba(1)–O(23)	88.2(3)
I(1)–Ba(1)–O(28)	89.2(3)	O(18)–Ba(1)–O(28)	89.0(4)
I(1)′–Ba(1)–O(2)	174.0(2)	O(23)–Ba(1)–O(28)	171.4(3)
I(1)′–Ba(1)–O(18)	74.1(2)	Ba(1)–I(1)–Ba(1)′	104.23(4)
I(1)′–Ba(1)–O(23)	91.3(2)	Ba(1)–O(2)–C(3)	177(1)
I(1)′–Ba(1)–O(28)	95.8(2)		

$$\mathrm{KOR + AeI_2 \xrightarrow{THF} IAe(OR)(THF)_{\mathit{n}} + KI\downarrow} \qquad (2)$$

$$\mathrm{Ae(OR)_2(THF)_3 + AeI_2 \xrightarrow{THF} 2IAeOR(THF)_{\mathit{n}}} \qquad (3)$$
$$\mathrm{Ae = Ca, Ba; OR = clox, BHT}$$

4). The white, crystalline compounds are stable in the absence of air and moisture.

$$\mathrm{2ICa(clox)(THF)_4 \overset{THF}{\nrightarrow} Ca(clox)_2(THF)_3 + CaI_2(THF)_{\mathit{n}}} \qquad (4)$$

Solution Behavior of 2. Mono(alkoxide) **2** displays indefinite stability in THF solution. In THF–d_8, the ^{1}H NMR of **2** exhibits the expected six peaks for the [clox]$^-$ ligand (H$_a$–H$_f$; see Figure 1); these resonances are distinct from those of Ca(clox)$_2$(THF)$_3$. This allows for unambiguous identification of the mono(alkoxide) (and any bis(alkoxide) impurity) in this solvent.

In toluene, **2** initially dissolves to form an almost clear solution (concentrations up to 3 mM are possible). However, over the course of a few hours, a white solid gradually precipitates from toluene solutions of **2**. ^{1}H NMR analysis (THF-d_8) of the precipitate formed after 24 h reveals it to be largely CaI$_2$(THF)$_n$. If the precipitated solid is removed by filtration, evaporation of the filtrate leaves a brown solid that contains crude [Ca(μ-clox)(clox)(THF)]$_2$;[5] the alcohol Hclox is the only identifiable impurity.

A ^{1}H NMR study revealed that a sample of **2** dissolved in C$_6$D$_6$ exhibits three separate sets of [clox]$^-$ resonances. One of these corresponds to the known compound Ca(clox)$_2$(THF)$_3$;[5] the other two sets have [clox]$^-$ phenyl proton resonances (H$_b$) at δ 7.79 and 7.51, with matching [clox]$^-$ methylene peaks (H$_a$) at δ 4.15 and 3.65 ppm, respectively (see assignments in Figure 1). These two set of resonances account for ca. 90% of the total intensity seen in the spectrum upon preparation. The downfield set of resonances, δ 7.79 and 4.15 ppm (**2a**), decreases in intensity relative to the δ 7.51/3.65 set (**2b**) as the initial concentration of **2** is increased. The concentration dependence seen above suggests that **2a** and **2b** are two distinct [clox]$^-$-containing compounds.

Repeated attempts to quantify accurately the time/concentration behavior of the solutions were frustrated by the low solubility of **2** in C$_6$D$_6$. Nevertheless, C$_6$D$_6$ solutions of **2** monitored over time revealed that the relative concentrations of **2a** and **2b**, often initially different, gradually changed on standing, so that after ca. 48 h the two species would be present in roughly equal amounts. This behavior implies that interconversion occurs between **2a** and **2b** in solution. The *total* concentration of **2a** and **2b** gradually decreases on standing. This decrease is mirrored by an increase in the concentration of Ca(clox)$_2$(THF)$_3$; however, even after 48 h the resonances of Ca(clox)$_2$(THF)$_3$ account for only about one-third of the total [clox]$^-$ resonances seen in the spectrum. Interestingly, resonances for **2a** and **2b** are not seen in the solid isolated from toluene solutions of **2**; it appears that these intermediates are completely decomposed when the solvent and additional coordinated THF are removed.

Solution Behavior of 4. The ^{1}H NMR spectrum (THF-d_8) of [IBa(BHT)(THF)$_3$]$_2$ is identical with that of Ba(BHT)$_2$(THF)$_3$.[5] These resonances are different from those seen for KBHT in d$_8$-THF (i.e., δ 6.57, 2.05, and 1.40 ppm), however, reducing the likelihood that the similarity of the spectra of **4** and Ba(BHT)$_2$(THF)$_3$ stems from the presence of solvent-separated [BHT]$^-$ anions.

Unlike Ba(BHT)$_2$(THF)$_3$, which is soluble in toluene,[21] a turbid suspension forms when **4** is added to toluene. The suspension thickens to form a gel on prolonged stirring; filtering gives a clear toluene filtrate and an off-white gel-like precipitate. Surprisingly, no solid is isolated on removal of the toluene from the filtrate. The lack of any toluene-soluble product from the toluene suspension indicates that **4** is completely insoluble in this solvent; hence, decomposition of **4** to produce Ba(BHT)$_2$(THF)$_x$ complexes by disproportionation does *not* occur. The precipitate dries under vacuum to a dense, hard gray solid (**5**). A THF-d_8 ^{1}H NMR spectrum of **5** exhibits three BHT peaks at the same location as those in both **4** and Ba(BHT)$_2$(THF)$_3$; nonstoichiometric amounts of toluene are also evident in the NMR spectrum. However, there are no peaks corresponding to coordinated protio-

---

[21] For example, 0.90 g of Ba(BHT)$_2$(THF)$_3$ can be dissolved in 20 mL of toluene to give a slightly cloudy solution. Stirring the solution for 48 h does not result in the formation of any precipitate. Removal of the toluene under vacuum yields 0.69 g of a cream powder that is still soluble in aromatics and displays a set of BHT resonances in its NMR spectrum (C$_6$D$_6$) that is different from that of Ba(BHT)$_2$(THF)$_3$. We have not been able to characterize this compound definitively; it may be a partially desolvated or oligomerized bis(alkoxide) complex such as [Ba(BHT)$_2$(THF)$_n$]$_x$ ($n < 3$, $x \geq 1$).

THF in the spectrum; this indicated that **5** is unsolvated, oligomeric $[\mathrm{IBa(BHT)}]_n(\mathrm{C_7H_8})_x$ (eq 5). An IR spectrum of **5** helps to

$$\mathrm{IBa(BHT)(THF)_3} \xrightarrow[-3\,\mathrm{THF}]{\text{toluene}} \xrightarrow{\text{vacuum}} [\mathrm{IBa(BHT)}]_n(\mathrm{C_7H_8})_x \quad (5)$$

confirm its assignment as the completely desolved mono(alkoxide); it qualitatively resembles that of $[\mathrm{IBa(BHT)(THF)_3}]_2$, except for the absence of bands at 1198, 880, and 819 $\mathrm{cm^{-1}}$ assignable to THF. Extended drying under vacuum does not completely remove the toluene; it evidently is strongly held in the lattice.

It is not known whether the THF is lost from the mono(aryloxide) as it is stirred in toluene or as it is dried under vacuum or if both steps contribute to the desolvation of the compound. Proton NMR spectra of **4** in $\mathrm{C_6D_6}$ confirm the results of the bulk toluene trituration, as the compound forms a turbid suspension in $\mathrm{C_6D_6}$, and the spectrum is essentially featureless. Such spectra thus can be used for unambiguous verification of pure, $\mathrm{Ba(BHT)_2(THF)_x}$-free samples of **4**, although it is still not possible to determine the relative concentrations of mixtures of **4** and $\mathrm{Ba(BHT)_2(THF)_x}$ by NMR.[22]

Derivatization of the Mono(alkoxides). Reaction of **2** with 1 equiv of Kclox in THF generates the homoleptic bis(alkoxide) $\mathrm{Ca(clox)_2(THF)_3}$ in 76% yield (eq 6). An analogous reaction of

$$\mathrm{ICa(clox)(THF)_4 + K(clox)} \xrightarrow{\mathrm{THF}} \mathrm{Ca(clox)_2(THF)_3 + KI}\downarrow \quad (6)$$

$$1/2[\mathrm{IBa(BHT)(THF)_3}]_2 + \mathrm{K(BHT)} \xrightarrow{\mathrm{THF}} \mathrm{Ba(BHT)_2(THF)_3 + KI}\downarrow \quad (7)$$

4 with KBHT in THF produces $\mathrm{Ba(BHT)_2(THF)_3}$ in 87% yield (eq 7). The bis(alkoxide) products are easily identified by their ^{1}H NMR spectra.[5]

Reaction of **2** with 1 equiv of $\mathrm{KN(SiMe_3)_2}$ in THF yields the colorless, crystalline compound $\mathrm{(clox)Ca[N(SiMe_3)_2](THF)_3}$ (**3**), the first amidoalkoxide of a heavy alkaline-earth metal (eq 8).

$$\mathrm{ICa(clox)(THF)_4 + KN(SiMe_3)_2} \xrightarrow{\mathrm{THF}} \mathrm{(clox)Ca[N(SiMe_3)_2](THF)_3 + KI}\downarrow \quad (8)$$

Like the mono(alkoxide) halides **2** and **4**, **3** is stable toward disproportionation in THF solution. However, **3** cannot be formed by the conproportionation route used for **2** and **4**; i.e., the reaction of $\mathrm{Ca(clox)(THF)_3}$ and $\{\mathrm{Ca[N(SiMe_3)_2]_2}\}_2$ does not form **3** in THF. The ^{1}H and ^{13}C NMR spectra of **3** in THF-d_8 show added complexity compared to those of **2**, with two sets of $[\mathrm{clox}]^-$ ligand resonances (cf. the single set of $[\mathrm{clox}]^-$ peaks seen in the spectrum of **2**) and two amido methyl resonances in both spectra.

The ^{1}H NMR spectrum of **3** in $\mathrm{C_6D_6}$ is also complex, with at least two distinct sets of $[\mathrm{clox}]^-$ resonances and four different methyl resonances for the $[\mathrm{N(SiMe_3)_2}]^-$ ligand. Additionally, there is a pronounced concentration dependence seen in the spectra of **3**; as the concentration of **3** is increased, one set of $[\mathrm{clox}]^-$ resonances and two sets of the amido methyl resonances (**3a**) increase in intensity compared to the remaining resonances (**3b**) (see Experimental Section). Resonances corresponding to the homoleptic complexes $\mathrm{Ca(clox)_2(THF)_3}$ and $\mathrm{Ca[N(SiMe_3)_2]_2(THF)_2}$ are always present in variable amounts in the NMR spectra ($\mathrm{C_6D_6}$) of **3**, even in solutions prepared from crystalline samples. However, these resonances are never present in more than ca. 5% of the total intensity of the **3a** and **3b** peaks. This suggests that the equilibrium between **3**, $\mathrm{Ca(clox)_2(THF)_3}$, and $\mathrm{Ca[N(SiMe_3)_2]_2(THF)_2}$ in aromatic solution lies strongly in favor of the heteroleptic compound.

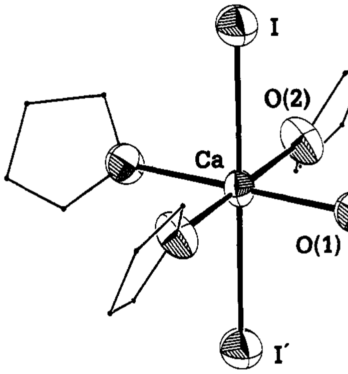

Figure 2. ORTEP diagram of the non-hydrogen atoms of **1**, illustrating the numbering scheme used in the text. Thermal ellipsoids are shown at the 35% level, and the carbon atoms are represented as dots.

Solid-State Structures $\mathrm{CaI_2(THF)_4}$ (1). As the alkaline-earth diiodides serve as the ultimate starting materials for the compounds described here, we investigated the structure of THF-solvated $\mathrm{CaI_2}$. The material that results on recrystallization of anhydrous $\mathrm{CaI_2}$ from THF has the formula $\mathrm{CaI_2(THF)_4}$.[18]

Unsolvated $\mathrm{CaI_2}$ is a nonmolecular material that crystallizes with a $\mathrm{CdI_2}$ lattice.[23] In contrast, $\mathrm{CaI_2(THF)_4}$ exists as a monomeric species with a distorted octahedral geometry, isostructural with the tetrahydrates $\mathrm{CaI_2(H_2O)_4}$[24] and $\mathrm{CaCl_2(H_2O)_4}$.[25] The same geometry is also found in the calcium tellurolate complex $\mathrm{Ca[TeSi(SiMe_3)_3]_2(THF)_4}$[26] and in solvated magnesium dihalides such as $\mathrm{MgCl_2(py)_4}$[27] and $\mathrm{MgBr_2(py)_4{\cdot}2py}$.[28]

The oxygen atoms of four THF molecules lie in a plane around the calcium atom, and the iodide atoms lie directly above and below the plane (Figure 2). Only half the molecule is unique, as the calcium atom lies on an inversion center. The *cis* ligand–metal–ligand angles are in the range 89–91°, and the *trans* angles are necessarily 180°. The metal–iodide and metal–oxygen distances are 3.106(2), and 2.33(1) and 2.35(1) Å, respectively. There is disorder associated with the THF groups that makes them appear planar; this probably does not affect the Ca–ligand bond lengths (cf. the Ca–THF distances of 2.34(1) Å in the six-coordinate complex $\{[(i\text{-Pr})_4\mathrm{C_5H}]\mathrm{CaI(THF)}\}_2$[29]). These distances are somewhat shorter than those found in the calcium alkoxide compounds $\mathrm{Ca(BHT)_2(THF)_3{\cdot}(THF)}$ (2.39 Å) and $[\mathrm{Ca(\mu\text{-}clox)(clox)(THF)}]_2$ (2.41 Å), even though the coordination number of calcium is lower in the latter complexes.[5]

$\mathrm{ICa(clox)(THF)_4}$ (2). This mono(alkoxide) crystallizes as a monomeric complex with a distorted octahedral geometry. Somewhat surprisingly, the replacement of $\mathrm{I^-}$ with a $[\mathrm{clox}]^-$ ligand on going from **1** to **2** occurs without changing the octahedral geometry at the calcium atom. Unlike the arrangement in **1**, however, the anionic groups in **2** are in a *cis* configuration (Figure 3). The calcium–iodide distance of 3.108(3) Å in **2** is indistinguishable from that in **1**. The calcium–THF distances in **2** range from 2.391(9) to 2.454(9) Å, somewhat longer (by 0.06–0.10 Å) than those in **1**. The Ca–O alkoxide bond distance (2.097(7) Å) is nearly identical with those seen in $[\mathrm{Ca(\mu\text{-}clox)(clox)(THF)}]_2$ (2.105(2) Å (terminal)) and $\mathrm{Ca(clox)_2(THF)_3{\cdot}(THF)}$ (2.08(2) and 2.07(2) Å),[5] despite the higher metal coordination number in **2**. As is often found in alkaline-earth alkoxides, the Ca–O–

---

[22] A ^{1}H NMR spectra of a known 1:1 mixture of **4** and $\mathrm{Ba(BHT)_2(THF)_3}$ in THF-d_8 still displays only three distinct singlets at 6.68, 2.09, and 1.43 ppm, besides the coordinated THF peaks. No differentiation or even a noticeable broadening of the peaks is seen.

(23) Wells, A. F. *Structural Inorganic Chemistry*, 5th ed.; Clarendon: Oxford, U.K., 1984; p 415.

(24) Thiele, G.; Putzas, D. *Z. Anorg. Allg. Chem.* **1984**, *519*, 217–224.

(25) Leclaire, A.; Borel, M. M.; Monier, J. C. *Acta Crystallogr., Sect. B* **1980**, *36*, 2757–2759.

(26) Gindelberger, D. E.; Arnold, J. *J. Am. Chem. Soc.* **1992**, *114*, 6242–6243.

(27) Halut-Desportes, S.; Bois, C. *Acta Crystallogr., Sect. B* **1979**, *35*, 2205–2207.

(28) Halut-Desportes, S. *Acta Crystallogr., Sect. B* **1977**, *33*, 599–601.

(29) Burkey, D. J.; Alexander, E. K.; Hanusa, T. P. Submitted for publication.

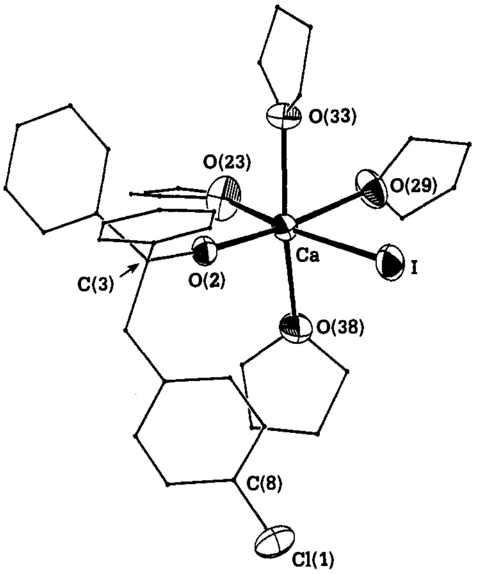

Figure 3. ORTEP diagram of the non-hydrogen atoms of **2**, illustrating the numbering scheme used in the text. Thermal ellipsoids are shown at the 30% level, and the carbon atoms are represented as dots.

C(3) angle in **2** is almost linear (172.9(6)°). This value does not necessarily imply any degree of M–O–C multiple bonding, however.[5]

We were initially intrigued by the *cis* arrangement of anionic ligands around the calcium atom, as all other calcium complexes of this type $[Ca(X)_2(L)_n]$ (X = anionic ligand, $n > 3$) exhibit a *trans* geometry, presumably to minimize anion–anion repulsion.[30] A superficially appealing explanation for the *cis* arrangement of anionic ligands in **2** is the steric relief that might be gained from placing the bulky [clox]$^-$ ligand next to the sterically compact iodide (van der Waals radius = 2.15 Å[31]). However, the crystallographically characterized cation of a similar monomeric d^0 mono(alkoxide) halide, $[Y(OCMe_3)Cl(THF)_5][BPh_4]$,[32] has an yttrium atom coordinated by a *tert*-butylalkoxide and a chloride ligand in a *trans* geometry, with *five* THF ligands coordinated in a plane around the yttrium atom, all *cis* to the bulky *tert*-butoxy ligand. Justifying the *cis* arrangement of ligands in **2** on steric grounds may thus not be valid. Other, more subtle factors such as crystal packing forces must therefore be responsible for the observed *cis* geometry of **2**. If so, this indicates that a small energy difference exists between the two possible geometries, a finding in line with recent ab initio calculations on an analogous model calcium complex $[Ca(NH_2)_2(HF)_4]$, which detected only a small (<1 kcal mol^{-1}) energy difference between the *cis* and *trans* geometries.[30] It then becomes an interesting question why more calcium complexes of this type have not been isolated with *cis* geometries; this point may bear further investigation.

(clox)Ca[N(SiMe$_3$)$_2$](THF)$_3$ (3). The X-ray crystal structure determination of **3** is the first for a heteroleptic calcium compound with an alkoxide ligand. It is monomeric in the solid state, with the ligands in a distorted TBP geometry (Figure 4). The two anionic ligands occupy equatorial sites, with the three THF's in the remaining positions. This geometrical arrangement of ligands has previously been seen in the bis(alkoxide) complex $Ca(clox)_2(THF)_3$[5] and also in several alkaline-earth aryloxides.[4,33]

$Ca(clox)_2(THF)_3$ and **3** have strikingly similar structural parameters. To begin with, the metal–alkoxide distances of 2.097(7) Å in **3** and 2.08(2) and 2.09(2) Å in $Ca(clox)_2(THF)_3$ are equivalent within error. Both the angle between the anionic ligands (124.2(2)° vs 126°) and the axial THF–Ca–THF angle (159.1(2)° vs 163°) in the two complexes are also nearly identical. Apparently the change from two [clox]$^-$ ligands in $Ca(clox)_2(THF)_3$ to a [clox]$^-$ and a $[N(SiMe_3)_2]^-$ ligand in **3** can be accommodated without requiring major structural reorientations around the calcium atom; in this case, these ligands can be considered isosteric.

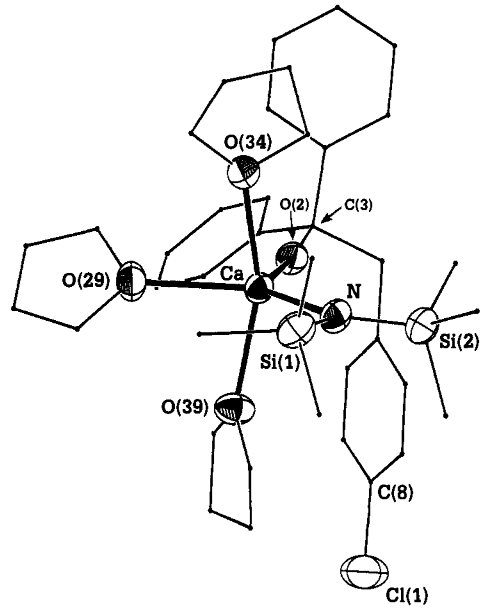

Figure 4. ORTEP diagram of the non-hydrogen atoms of **3**, illustrating the numbering scheme used in the text. Thermal ellipsoids are shown at the 30% level, and the carbon atoms are represented as dots.

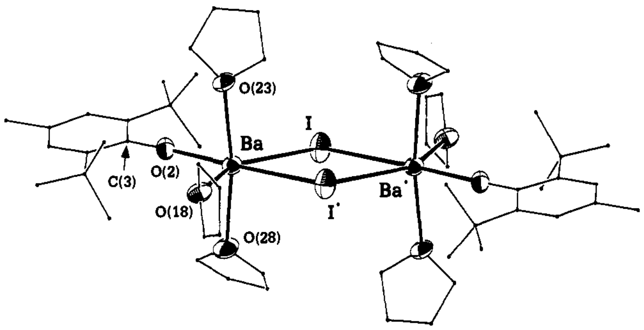

Figure 5. ORTEP diagram of the non-hydrogen atoms of **4**, illustrating the numbering scheme used in the text. Thermal ellipsoids are shown at the 50% level, and the carbon atoms are represented as dots. The lattice solvent has been omitted for clarity.

The Ca–N bond distance of 2.353(5) Å in **3** can be compared to that in the two other structurally characterized Ca amido compounds, $\{Ca[N(SiMe_3)_2]_2\}_2$ and $Ca[N(SiMe_3)_2]_2(DME)$,[34] both of which have shorter Ca–N distances. In $\{Ca[N(SiMe_3)_2]_2\}_2$, the two terminal Ca–N distances are 2.282(6) and 2.267(7) Å, and in $Ca[N(SiMe_3)_2]_2(DME)$, the terminal Ca–N distance is 2.271(3) Å. A longer Ca–N bond in **3** is reasonable on the basis of its higher calcium coordination number (5) compared to that of the bis(amido) compounds.

[IBa(BHT)(THF)$_3$]$_2$·(THF)$_2$ (4). The second iodoalkoxide **4** crystallizes from THF as an asymmetrically bridged dimer, in which each Ba atom is coordinated by three THF's, a terminal BHT ligand, and two bridging iodide ligands (Figure 5). Together, the ligands define two edge-sharing distorted octahedra; an inversion center at the middle of the Ba_2I_2 core relates the two asymmetric units. One lattice THF in the asymmetric unit (two per dimer) completes the structure.

The metal–iodide distances are 3.443(2) and 3.590(2) Å, *cis* and *trans* to the aryloxide ligand, respectively. The asymmetry

---

(30) Mösges, G.; Hampel, F.; Kaupp, M.; Schleyer, P. v. R. *J. Am. Chem. Soc.* **1992**, *114*, 10880–10889.

(31) Pauling, L. *The Nature of the Chemical Bond*, 3rd ed.; Cornell University Press: Ithaca, NY, 1960; p 260.

(32) Evans, W. J.; Olofson, J. M.; Ziller, J. W. *J. Am. Chem. Soc.* **1990**, *112*, 2308–2314.

(33) Hitchcock, P. B.; Lappert, M. F.; Lawless, G. A.; Royo, B. *J. Chem. Soc., Chem. Commun.* **1990**, 1141–1142.

(34) Westerhausen, M.; Schwarz, W. *Z. Anorg. Allg. Chem.* **1991**, *604*, 127–140.

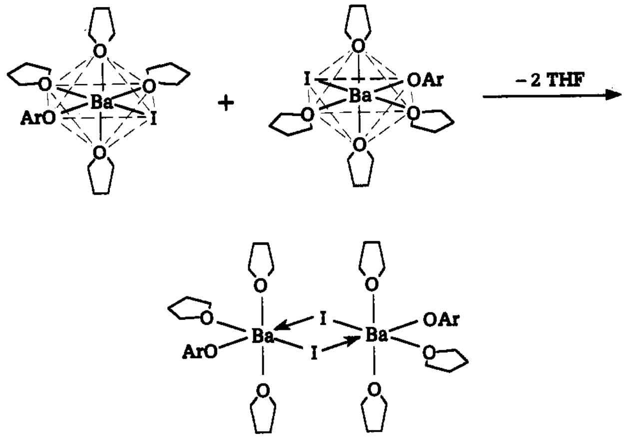

Figure 6. Conjectural formation of 4 from two *cis* IBa(BHT)(THF)$_4$ complexes.

parameter (ϕ) for the dimer is 6.8%, which is toward the high end of the range of values (from 2.9 to 8.1%) found for ϕ in various other alkaline-earth and lanthanide dimers.[18] Since the shorter Ba–I bond is *cis* to the terminal [BHT]$^-$ ligand, the dimer can be thought of (in a structural, and not necessarily a mechanistic sense) as formed from two monomeric "IBa(BHT)(THF)$_4$" species (with the same *cis* geometry of anionic ligands as seen in 2) that have condensed to form a dimer with loss of the THF *trans* to the [BHT]$^-$ ligand from each Ba atom (Figure 6).

The metal–aryloxide bond distance is 2.405(8) Å; this distance falls between the two analogous Ba–O distances in Ba(BHT)$_2$(THF)$_3$ (2.38(1) and 2.42(1) Å).[5] The coordinated THF molecules lie 2.69(1), 2.695(9), and 2.71(1) Å from the metal center; these Ba–O distances are comparable to those found in Ba(BHT)$_2$(THF)$_3$ (2.72(1)–2.75(1) Å).

Discussion

Formation and Stability of Mono(alkoxide) Halides of the Heavy Alkaline-Earth Metals. Almost all previous research on the synthesis of molecular alkaline-earth alkoxides has been on homoleptic bis(alkoxide) complexes of the type [Ae(OR)$_2$(L)$_n$]. Until now, controlled manipulation of the properties of these complexes has focused on changing the nature of the alkoxide ligand (i.e., using sterically bulky or potentially chelating R groups) and/or changing the number and type of neutral bases (L) coordinated to the metal center.[4,5] The [Ae(OR)X(L)$_n$] complexes decribed here illustrate an alternate and potentially more flexible means of producing alkaline-earth alkoxide complexes with desirable properties.

The mono(alkoxide) iodide complexes 2 and 4 were synthesized by means of metathesis and conproportionation reactions involving the alkaline-earth diiodides. Our choice of halide-containing precursors was designed to provide greater control of the stoichiometry of reactions than could be had starting from the metal and the appropriate alcohols. The success of these reactions is owed to the complete stability of 2 and 4 in THF solution; no complications arising from disproportionation of the mono(alkoxides) via Schlenk equilibria are observed in the solvent. The stability of 4 is especially notable in that disporportionation to give the soluble bis(aryloxide) and at least partial precipitation of the only slightly THF-soluble BaI$_2$ would seem to be a favorable process (eq 9).

$$2\mathrm{IBa(BHT)(THF)_3} \overset{\mathrm{THF}}{\nrightarrow} \mathrm{Ba(BHT)_2(THF)_3} + \mathrm{BaI_2}\downarrow \quad (9)$$

With only two characterized examples, it is not yet possible to say that the THF stability of 2 and 4 demonstrates that mono(alkoxide) halide complexes of Ca, Sr, and Ba will in general be stable toward disproportionation in this solvent. It should be noted that the solution stability of analogous tin mono(alkoxide) halide complexes in ethers is highly dependent on the nature of the alkoxide group. For example, SnCl$_2$ and KO-*t*-Bu react at –60 °C in THF to form [SnCl(O-*t*-Bu)]$_2$·THF; above –35 °C, however, the mono(alkoxide) dissociates into SnCl$_2$ and Sn(O-t-Bu)$_2$.[35] In contrast, it has been reported that Sn(OMe)$_2$ and SnX$_2$ (X = Cl, Br, I) conproportionate at room temperature in THF to form stable SnX(OMe) complexes.[36]

In aromatic solvents, an unexpectedly complex solution behavior is displayed by the mono(alkoxide) complex 2. The compound is modestly soluble in aromatic solvents, but upon dissolution it immediately begins to disporportionate to form CaI$_2$(THF)$_x$ and the known bis(alkoxide) Ca(clox)$_2$(THF)$_3$. However, this decomposition occurs primarily through *two* different intermediate species (2a and 2b) that can be seen in the NMR spectra of 2 in C$_6$D$_6$. Although we have no definite evidence for the composition of these intermediates, they are most likely complexes of the type [ICa(clox)(THF)$_n$]$_x$, where $n < 4$ and $x \geq 2$, with either bridging I$^-$ or [clox]$^-$ ligands. Precedence for this type of geometry is found in the related solid-state structure of 4. The decomposition is also remarkably slow, as both intermediates account for over half the [clox]$^-$-containing compounds present in solution ca. 2 days after dissolution, even though decomposition to produce Ca(clox)$_2$(THF)$_3$ is irreversible owing to the precipitation of CaI$_2$(THF)$_x$.

Almost exactly the opposite solution behavior is shown by 4 in aromatics. It is completely insoluble in toluene and so does not undergo decomposition but is simply desolvated by the combination of toluene trituration and vacuum drying to form the presumably polymeric material [IBa(BHT)]$_n$(C$_7$H$_8$)$_x$. A higher degree of unsaturation at the metal center in 4 and a greater ease of THF removal from it are likely contributors to the widely different toluene solubilities of the two mono(alkoxides). The ease of removal of THF from barium compounds compared to their calcium counterparts has been noted before and attributed to the lower Lewis acidity of Ba^{2+} relative to Ca^{2+}.[17,37]

The solution behavior of 2 and 4 contrasts with that of Cp*CaI(THF)$_2$, which is relatively stable toward disproportionation in aromatic solutions ($K_{eq} = 1.7 \times 10^{-3}$).[18] It is scrambled in THF solution, however, giving a statistical distribution of Cp*$_2$Ca(THF)$_2$, Cp*CaI(THF)$_2$, and CaI$_2$(THF)$_n$. Derivatization reactions of Cp*CaI(THF)$_2$ must therefore be conducted in toluene. The solution stability of the mono(alkoxides) is the inverse; i.e., derivatization reactions with these compounds must be conducted in THF and not aromatics. These two classes of mono(halide) alkaline-earth compounds thus complement each other in the conditions required for derivatization reactions. They also illustrate the substantially different effects that cyclopentadienyl and alkoxide ligands have on the properties of alkaline-earth compounds.

The mono(alkoxide) amido complex 3 is stable toward disproportionation in THF. However, surprisingly complexity is seen in its THF-d_8 NMR spectra, as two distinct sets of resonances for both the [clox]$^-$ and [N(SiMe$_3$)$_2$]$^-$ ligands are observed. This complexity can be accounted for by the presence of two inequivalent ligand environments in solution, although the process by which they arise is not known.

Like Cp*CaI(THF)$_2$, 3 is modestly stable toward disproportionation in aromatic solution, with the corresponding homoleptic species present in minor amounts. Interestingly, similar stability in aromatic solution has been reported for tin and zinc analogues of 3, [Sn(N(SiMe$_3$)$_2$)(μ-O-*t*-Bu)]$_2$[10] and [Zn(N(SiMe$_3$)$_2$)(μ-O-*t*-Bu)]$_2$.[38]

Metal–Iodide Interactions. As the iodide ligand occurs in the starting materials for these compounds (CaI$_2$, BaI$_2$) and in two

---

[35] Zybill, C.; Müller, G. *Z. Naturforsch., B*: *Anorg. Chem.* **1988**, *43*, 45–48.

[36] Ewings, P. F. R.; Harrison, P. G. *J. Chem. Soc., Dalton Trans.* **1975**, 1717–1721.

[37] Gardiner, M. G.; Raston, C. L.; Kennard, C. H. L. *Organometallics* **1991**, *10*, 3680–3686.

[38] Goel, S. C.; Chiang, M. Y.; Buhro, W. E. *Inorg. Chem.* **1990**, *29*, 4646–4652.

Table 6. Comparison of Effective Iodide Radii (Å) in Alkaline-Earth and f-Element Complexes

metal–iodide complex	M–I distance[a] (Å)	CN at M	metal radius[b]	effective iodide radius[c]	ref
Terminal Iodides					
$CaI_2(THF)_4$	3.106(2)*	6	1.00	2.11	this work
$CaI_2(H_2O)_4$	3.127(7)*	6	1.00	2.13	24
$ICa(clox)(THF)_4$	3.108(3)	6	1.00	2.11	this work
$Cp^*CeI_2(THF)_3$	3.2269(12)	8	1.143	2.084	53
	3.1733(12)			2.030	
$Cp^*_2CeI(N{\equiv}CCH_3)_2$	3.231(2)	9	1.196	2.035	54
$[SmI_2(THF)_5]^+[Co(CO)_4]^-$	3.009(2)	7	1.02	1.99	51
	3.030(2)			2.01	
$Cp^*_2SmI(THF)$	3.043(2)	8	1.08	1.96	55
	3.053(2)			1.97	
cis-$SmI_2[O(CH_2CH_2OMe)_2]_2$	3.322(1)	8	1.27	2.05	63
	3.333(1)	8	1.27	2.06	
trans-$SmI_2[O(CH_2CH_2OMe)_2]_2$	3.265(1)	8	1.27	2.00	63
$Cp^*_2SmI(\eta^2\text{-}N_4C_6H_{10})$	3.100(2)	9	1.13	1.97	56
$Cp^*_2Th(I)Ru(Cp)(CO)_2$	3.0435(6)	8	1.05	1.99	59
$UI_3(THF)_4$	3.102(2)	7	1.07	2.03	58
	3.167(2)			2.10	
	3.119(2)			2.05	
$[MeO(CH_2)_2C_5H_4]_2YbI$	3.049(1)	9	1.042	2.007	57
μ_2-Iodides					
$[IBa(BHT)(THF)_3{\cdot}THF]_2$	3.433(2)	6	1.35	2.08	this work
	3.590(2)			2.24	
$[Cp^*CaI(THF)_2]_2$	3.1283(15)	7	1.06	2.07	18
	3.1356(15)			2.08	
	3.1980(16)			2.14	
	3.2743(16)			2.21	
$[SmI_2(N{\equiv}CCMe_3)_2]_n$	3.260(1)	6	1.17	2.09	64
	3.225(1)	6	1.17	2.06	
$[Cp^*SmI(THF)_2]_2$	3.356(2)	7	1.22	2.14	61
	3.459(2)			2.24	
$\{[(Me_3Si)_2N]_2SmI(DME)(THF)_2\}_2$	3.3414(9)	8	1.079	2.262	62
	3.3553(9)			2.276	
$Li[Cp^*YbI_2](ether)_2$	3.027(1)*	8	0.985	2.042	60

[a] Starred compounds have two crystallographically equivalent M–I distances. [b] Shannon radii. [c] Calculated by subtracting the metal radius from the metal–iodide bond distance.

of the mono(alkoxides), it is instructive to make a comparison of the metal–iodide distances with those in iodo complexes of other electropositive, d^0 metals. This can be done with the use of "effective radii", which have been calculated for oxygen and halide ligands in lanthanide and alkaline-earth complexes by subtracting the metal radii values (adjusted for coordination number and oxidation state) from the observed metal–ligand distances.[5,39,40]

Comparisons are made between several alkaline-earth and f-block d^0 iodo compounds and **1**, **2**, and **4** in Table 6. The average effective iodide radii for terminal iodides is 2.04 Å, but individual values range from 1.96 to 2.13 Å. There is no obvious correlation of the values with metal type or oxidation state. The variation of values observed for the three independent U–I distances in $UI_3(THF)_4$ (2.03, 2.05, and 2.10 Å) underscores the variability of the calculated radii. Large variations are also observed in the calculated radii for bridging iodides; these differences might reflect differences between bonding modes (i.e., "primary" and "secondary" (dative) bonding[41,42]).

An alternate measure of the internal consistency of the data can be obtained from plots of terminal metal–iodide distances vs metal radii. If the effective iodide radii were constant, such a plot should have a slope of unity (i.e., $dR_{M-I}/dr_{M^+} = 1$).[43] The data in Table 6 correlate poorly in such a plot (Figure 7); the least-squares slope is 0.82 with $r^2 = 0.72$. Similar deviations in the slope and correlation observed in a plot of metal–Cp distances for the first row d-block metallocenes ($dR_{M-C}/dr_+ = 1.18$; $r^2 = 0.83$) were taken as structural evidence that the compounds did *not* fit an ionic model.[22,44] In contrast to both these classes of compounds, a recent study of effective oxygen radii in lanthanide alkoxides found that they did approach the ionic limit ($dR_{M-OR}/dr_+ = 0.93$; $r^2 = 0.91$).[40]

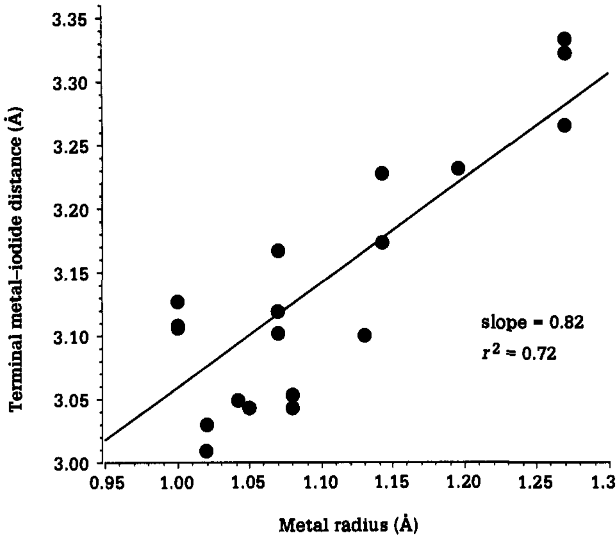

Figure 7. Scatter plot of metal–iodide distances vs metal radii in d^0 alkaline-earth and f-element complexes. The line is the linear least-squares fit to the data; the slope is 0.82, and $r^2 = 0.72$.

This analysis points out the often overlooked fact that calculated Shannon radii of metal ions are based primarily on distances in metal oxides and fluorides.[45] Although these radii have been used successfully to rationalize the distances in many coordination and organometallic compounds, it is not surprising that they do

---

(39) Evans, W. J.; Peterson, T. T.; Rausch, M. D.; Hunter, W. E.; Zhang, H.; Atwood, J. L. *Organometallics* **1985**, *4*, 554–559.

(40) Herrmann, W. A.; Anwander, R.; Scherer, W. *Chem. Ber.* **1993**, *126*, 1533–1539.

(41) Alcock, N. W. *Adv. Chem. Radiochem.* **1972**, *15*, 1–58.

(42) Haaland, A. *Angew. Chem., Int. Engl. Ed.* **1989**, *28*, 992–1007.

(43) Sockwell, S. C.; Hanusa, T. P. *Inorg. Chem.* **1990**, *29*, 76–80.

(44) Raymond, K. N.; Eigenbrot, C. W. *Acc. Chem. Res.* **1980**, *13*, 276–283.

(45) Shannon, R. D. *Acta Crystallogr., Sect. A* **1976**, *A32*, 751–767.

not adequately predict metal–ligand distances when highly polarizable anions such as I^- are involved.

Coordination Number and Electronic Saturation. Attempts at rationalizing the composition and structures of lanthanide and actinide compounds have frequently stressed the importance of maximizing electrostatic interactions and minimizing interligand repulsions.[46] Although both cation/anion attractions and the coordination of neutral bases to metal centers rely on electrostatic forces, the number and binding strength of binding of neutral ligands often have been analyzed primarily in terms of steric effects.[47,48] Thus for example, the tendency of complexes such as $Cp_2UCl_2(L)_2$ to extrude their coordinated bases spontaneously has been cited as an example of steric oversaturation of the metal.[49,50] The structures of the alkaline-earth diiodides and mono(alkoxides) reported here suggest that both steric and nonsteric factors are of comparable importance in determining the number of neutral ligands in these divalent complexes.

Compound **1** crystallizes from THF as the tetrasolvate, so a steric-centered analysis might conclude that four is the maximum number of THF's that can bind to a metal center the size of a Ca^{2+} ion that already is coordinated by two iodides. A counterexample from lanthanide chemistry argues against this, however. The cation $[SmI_2(THF)_5]^+$ crystallizes from THF with two *trans* iodides and *five* THF's in the plane of the Sm atom.[51] As seven-coordinate Sm^{3+} is approximately the same size as six-coordinate Ca^{2+} (Shannon radii of 1.02 and 1.00 Å, respectively), it appears that another THF ligand could be coordinated to the calcium without undue steric crowding. Related evidence is provided by the structure of $MgBr_2(THF)_4$,[52] in which four THF molecules fit around the considerably smaller radius of Mg^{2+} (Mg^{2+} = 0.72 Å, Ca^{2+} = 1.00 Å).[45] The electron density from the ligands in **1** effectively balances the Lewis acidity of the Ca^{2+} so that the binding of a fifth THF ligand is not energetically favorable. The coordinative unsaturation in **1** is emphasized by the fact that both it and **2** have four THF's coordinated to calcium, even though an iodide in **1** has been formally replaced by the much bulkier [clox]$^-$ ligand in **2**.

The idea that an alkaline-earth complex might be "electronically saturated" by neutral ligands but remain sterically unsaturated can be used to rationalize the observed dimeric structure of **4**. A monomeric "IBaBHT(THF)$_n$" ($n \geq 4$) structure analogous to that of **2** would certainly be sterically allowed, given the large radius of Ba^{2+}. However, the binding of more than three THF's to the barium is apparently not favorable, as it would place too much electron density at the less acidic Ba^{2+} center. Therefore, only three THF's bind to the IBa(BHT) fragment; the resulting "IBa(BHT)(THF)$_3$" then dimerizes to form **4**. This suggests that the difficulty in forming monomeric barium alkoxides[5] may be more a consequence of the low Lewis acidity of Ba^{2+} (a function of the *charge* and radius) rather than the large size of the metal ion itself.

The above alkaline-earth compounds, all of which have only one (or no) bulky ligand(s), provide a set of complexes in which the influence of ligand steric effects evidently plays a secondary role to electrostatics in the determination of their solid-state structures. In particular, it seems that the number of coordinated neutral ligands is limited more by electronic factors than by steric crowding around the metal center. The lower Lewis acidity of the heavy group 2 metals is likely the fundamental source of this ligand limit, although the electron donation properties of the ligands also may play a role. For metals with higher Lewis acidity, like the tri- and tetravalent f-block elements, comparable electronic limits to the number of coordinated neutral ligands probably will be more difficult to observe.

Conclusions

Mono(alkoxide) halide complexes of calcium and barium have been formed by metathetical reactions between potassium alkoxides and alkaline-earth iodides, and by conproportionation reactions between alkaline-earth bis(alkoxides) and the diiodides. In THF, the mono(alkoxides) display high kinetic stability; in aromatic hydrocarbons, however, loss of THF produces widely different solution behavior, ranging from simple desolvation to decomposition. The derivatization reactions with either alkoxides or amides suggest that the mono(alkoxide) species may serve as an important new class of reagents in the synthesis of alkaline-earth complexes.

The composition and structural features of the compounds have also made more obvious the limited usefulness of coordination number in defining the stability of these compounds. They also emphasize how the Lewis acidity of the metal center plays a central role in moderating the number of neutral ligands that can be coordinated to the metal. This seems to be an underappreciated design principle in alkaline-earth chemistry; its development and application should help expand the range of accessible mono(alkoxides) and other heteroleptic compounds for these elements.

Acknowledgment is made to the Donors of the Petroleum Research Fund, administered by the American Chemical Society, and to the University Research Council of Vanderbilt University for support of this research. D.J.B. is the recipient of an NSF Predoctoral Fellowship. We thank a reviewer for helpful comments. Funds for the X-ray diffraction facility at Vanderbilt University were provided through NSF Grant CHE-8908065.

Supplementary Material Available: Tables of fractional coordinates, bond distances and angles, and anisotropic thermal parameters (20 pages). This material is contained in many libraries on microfiche, immediately follows this article in the microfilm version of the journal, and can be ordered from the ACS; see any current masthead page for ordering information.

---

(46) Evans, W. J. *Adv. Organomet. Chem.* **1985**, *24*, 131–177.

(47) Xing-Fu, L.; Xi-Zhang, F.; Ying-Ting, X.; Hai-Tung, W.; Jie, S.; Li, L.; Peng-Nian, S. *Inorg. Chim. Acta* **1986**, *116*, 85–93.

(48) Xi-Zhang, F.; Ao-Ling, G.; Ying-Ting, X.; Xing-Fu, L. *Polyhedron* **1987**, *6*, 1041–1048.

(49) Bagnall, K. W.; Xing-Fu, L. *J. Chem. Soc., Dalton Trans.* **1982**, 1365–1369.

(50) Bagnall, K. W.; Velasquez, L. O.; Xing-Fu, L. *J. Chem. Soc., Dalton Trans.* **1983**, 1153–1158.

(51) Evans, W. J.; Bloom, I.; Grate, J. W.; Hughes, L. A.; Hunter, W. E.; Atwood, J. L. *Inorg. Chem.* **1985**, *24*, 4620–4623.

(52) Perucaud, M. C.; Le Bihan, M. T. *Acta Crystallogr., Sect. B* **1968**, *24*, 1502–1505.

(53) Hazin, P. N.; Huffman, J. C.; Bruno, J. W. *Organometallics* **1987**, *6*, 23–27.

(54) Hazin, P. N.; Lakshminarayan, C.; Brinen, L. S.; Knee, J. L.; Bruno, J. W.; Streib, W. E.; Folting, K. *Inorg. Chem.* **1988**, *27*, 1393–1400.

(55) Evans, W. J.; Grate, J. W.; Levan, K. R.; Bloom, I.; Peterson, T. T.; Doedens, R. J.; Zhang, H.; Atwood, J. L. *Inorg. Chem.* **1986**, *25*, 3614–3619.

(56) Evans, W. J.; Drummond, D. K.; Hughes, L. A.; Zhang, H.; Atwood, J. L. *Polyhedron* **1988**, *7*, 1693–1703.

(57) Deng, D.; Qian, C.; Song, F.; Wang, Z.; Wu, G.; Zheng, P.; Jin, S.; Lin, Y. *J. Organomet. Chem.* **1993**, *458*, 83–88.

(58) Clark, D. L.; Sattelberger, A. P.; Bott, S. G.; Vrtis, R. N. *Inorg. Chem.* **1989**, *28*, 1771–1773.

(59) Sternal, R. S.; Brock, C. P.; Marks, T. J. *J. Am. Chem. Soc.* **1985**, *107*, 8270–8272.

(60) Watson, P. L.; Whitney, J. F.; Harlow, R. L. *Inorg. Chem.* **1981**, *20*, 3271–3278.

(61) Evans, W. J.; Grate, J. W.; Choi, H. W.; Bloom, I.; Hunter, W. E.; Atwood, J. L. *J. Am. Chem. Soc.* **1985**, *107*, 941–946.

(62) Evans, W. J.; Drummond, D. K.; Zhang, H.; Atwood, J. L. *Inorg. Chem.* **1988**, *27*, 575–579.

(63) Sen, A.; Chebolu, V.; Rheingold, A. L. *Inorg. Chem.* **1987**, *26*, 1821–1823.

(64) Chebolu, V.; Whittle, R. R.; Sen, A. *Inorg. Chem.* **1985**, *24*, 3082–3085.